Makkonen, Lasse and Ylhäisi, Jussi S. and Törnqvist, Jouko and Dawson, Andrew and Räisänen, Jouni (2014) Climate change projections for variables affecting road networks in Europe. Transportation Planning and Technology, 37 (8). pp. 678-694. ISSN 1029-0354

CLIMATE CHANGE PROJECTIONS FOR VARIABLES AFFECTING ROAD NETWORK INFRASTRUCTURE IN EUROPE

Lasse Makkonen[1], Jussi Ylhäisi[2], Jouko Törnqvist[1], Andrew Dawson[3], Jouni Räisänen[2]

[1]VTT Technical Research Centre of Finland, P.O. Box 1000, FI-02044 VTT, Finland
[2]University of Helsinki, Department of Physics, P.O. Box 64, FI-00014 Helsinki, Finland
[3]The University of Nottingham, Nottingham Transportation Engineering Centre,
E-mails: [1] lasse.makkonen@vtt.fi; [1] jouko.tornqvist@vtt.fi; [2] jussi.ylhaisi@helsinki.fi; [2] jouni.raisanen@helsinki.fi; [3] andrew.dawson@nottingham.ac.uk

CLIMATE CHANGE PROJECTIONS FOR VARIABLES AFFECTING ROAD NETWORKS IN EUROPE

Abstract. Global climate change will affect road networks during this century. The effects will be different in various parts of the world due to differences in the local climate change and in the structure and properties of the roads. In this paper, climate change projections are presented for climate variables that are most likely to affect the long-term performance of road networks in Europe. We apply four regional climate simulations up until the year 2100 using two plausible future emission scenarios. The results show that the changing climate will require significant adaptation measures in the near future in order to maintain the operability of the European road network and the related infrastructure.

Keywords: Road network, Road structure, Climate change, Adaptation, Infrastructure

1 Introduction

All infrastructure including road networks will be affected by the projected anthropogenic climate change (e.g. Anon 2008). Changes in such factors as maximum temperatures and heavy precipitation will be the most prominent but also several other variables are important for various parts of the world. The structure and properties of the roads will be significant factors in determining the severity of the effects in each country.

Comprehensive understanding of the relevant changes in the climate is crucial in order to plan and implement the required adaptation measures in good time. This will be possible only by combining the knowledge of pavement damage mechanisms and projections of the future climate.

While a large number of studies have been made on the general aspects of climate change (e.g. Räisänen et al. 2004; Castro et al. 2007) and the changes in the extreme conditions (Makkonen et al. 2007) in Europe, less attention has been paid to the particular variables that are likely to affect the long-term performance of road networks.

In this paper, projections for such variables based on regional climate simulations are presented for Europe. In order to assess the uncertainty of the results, the simulations are driven using two plausible future emission scenarios and boundary conditions provided by two different global climate models.

2 Climate simulation method and data

2.1 Global models

Data from two global climate model simulations, the Hadley Centre HadAM3H and Max-Planck Institute ECHAM4/OPYC3 simulations, were used to drive the numerical regional climate model RCAO (Döscher et al. 2002). HadAM3H is a high-resolution (1.875° longitude x 1.25° latitude) atmosphere model (Gordon et al. 2000) for which the sea surface temperature and sea ice conditions were derived from observations and earlier lower-resolution coupled atmosphere-ocean simulations, as explained by Räisänen et al. (2004). ECHAM4/OPYC3 is a coupled atmosphere-ocean model with a resolution equivalent to a grid spacing of 2.8° longitude x 2.8° latitude (Roeckner et al. 1999).

The global climate models were first run from 1960 to 1990 using observed or estimated changes in the atmospheric composition. From 1990 on, the calculation was continued as two separate simulations using different scenarios of anthropogenic greenhouse gas and sulphur emissions as used by the Intergovernmental Panel on Climate Change (IPCC) - IPCC SRES A2 and B2 (Nakićenović et al. 2000; Solomon et al. 2007). Both the greenhouse gas and sulphur emissions are larger for A2 than B2, but for long-term changes in the radiation balance, the difference in the cumulative greenhouse gas emissions dominates. Thus, the simulated global warming and the general magnitude of other climate changes in the late 21st century are larger for the A2 than the B2 scenario.

For driving the regional climate model, 30-year periods from both the HadAM3H and MPI/ECHAM4/OPYC3 simulations, the "control run" (January 1961 to December 1990) and the "scenario run" (January 2071 to December 2100) were used. The 30-year annual global mean warming predicted by HadAM3H from 1961 - 1990 to 2071 - 2100 is 3.2 °C for scenario A2 and 2.3 °C for scenario B2. The corresponding warming predicted by ECHAM4/OPYC3 is 3.4 °C for A2 and 2.6 °C for B2. These values are in the midrange of the uncertainty

interval reported by Meehl et al. (2007). Taking into account a wider range of emission scenarios, model-specific climate sensitivities and uncertainties in the carbon cycle, they projected a global warming of 1.1 - 6.4 °C from 1990 to 2095.

2.2 The regional model

The Rossby Centre coupled regional climate model RCAO consists of the atmospheric model RCA2 (Bringfelt et al. 2001) and the Baltic Sea model RCO (Meier et al. 1999; Meier 2001). The atmospheric model RCA2 originates from version 2.5 of the HIRLAM model (Eerola et al. 1997), but includes many new parameterizations and other changes as explained in Räisänen et al. (2004) and Jones et al. (2004). RCA2 was run in a rotated longitude-latitude grid with a 0.44° (approximately 49 km) resolution in both horizontal directions and with 24 vertical levels in the atmosphere. The integration domain of RCAO covers an area of 106 × 102 grid squares (see Räisänen et al. 2004). The Baltic Sea model RCO was run with the horizontal resolution of 11 km and with 41 vertical levels (see Meier, 2001). The coupling procedure between RCA2 and RCO is described in Döscher et al. (2002).

In the following, the HadAM3H-driven RCAO simulations will be denoted as "Had" and the ECHAM4/OPYC3-driven simulations as "MPI". The control runs for 1961 - 1990 are denoted "RCA2" and the scenario runs for 2071 - 2100 with the A2 scenario by the abbreviation "A2", and the scenario runs with the B2 scenario by "B2".

Accordingly, four climate projections were obtained: Both emission scenarios A2 and B2 were applied for both Had-driven and MPI-driven regional climate simulations. Results for all these four projections are presented in this paper for one variable (freeze-thaw cycles) in order to give some indications of the differences caused by the uncertainty in the future emissions and caused by differences in the driving global climate models. In that connection, the four results are denoted as Had-RCA2 A2, Had-RCA2 B2, MPI-RCA2 A2 and MPI-RCA2 B2. Otherwise, the results are given as the mean of the four different simulations. These are denoted as "AB". Since there is no objective way to rate the quality or relevance of the four simulations, we consider that the mean of them, AB, is our "best estimate".

The variables used in the analysis vary in their temporal resolution. Daily values were used for maximum and minimum temperature, whereas for precipitation and instantaneous temperature the data used had a 6-hour resolution. The analysis was done for both the annual and the seasonal (winter DJF, spring MAM, summer JJA, autumn SON) values. The seasonal values are given as maps in this paper for one parameter (freeze-thaw cycles) and discussed for others.

3 Results

The maps of the simulated changes (Figs. 1 - 6) were produced at the Department of Physics, University of Helsinki. It should be noted that, in some cases (most notably, Fig. 2), spurious features are seen near the map boundaries. These are associated with the relaxation zone used to fit the RCAO simulated fields to the data from the driving global models.

Changes in the annual maximum temperature (Fig. 1) are here defined as the 30-year mean difference (2071 - 2100 minus 1961 - 1990) in the single highest maximum temperature of each year, which always occurs during the summer season. In all of the four simulations, the mean of which is shown in Fig. 1, the largest increases are found in Central and Southern Europe with maximum values over France and Germany, whereas temperature changes in Northern Europe are found to be smaller. The four simulations showed a relatively large influence of the driving global model on regional climate simulations. In the coupled-GCM *MPI*, the increase in sea surface temperatures over the Atlantic Ocean is much larger than in *Had*, and this most likely contributes to the larger increase in maximum temperatures over western and central Europe in the corresponding RCAO simulations.

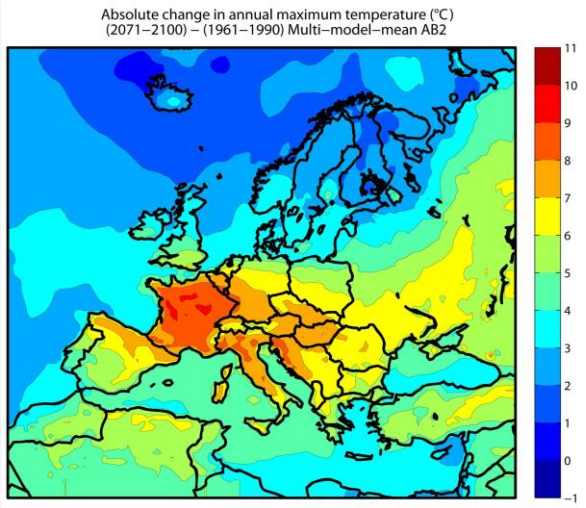

Fig. 1. Change in the annual maximum air temperature (°C)

Figure 2 shows the change in the annual number of events when the average air temperature changes by more than 15 °C in 6 hours. Note that the map does

not distinguish between cases of temperature increase and decrease. Most of the rapid, large temperature changes occur in the winter half-year in northern Europe and mountainous area (typically a few cases per year in the present climate) but in summer in the Mediterranean area (typically 20 - 40 cases). In western and central Europe, these large changes hardly exist. Consequently, the annual changes seen in Fig. 2 are dominated by the changes in north-eastern and Mediterranean Europe.

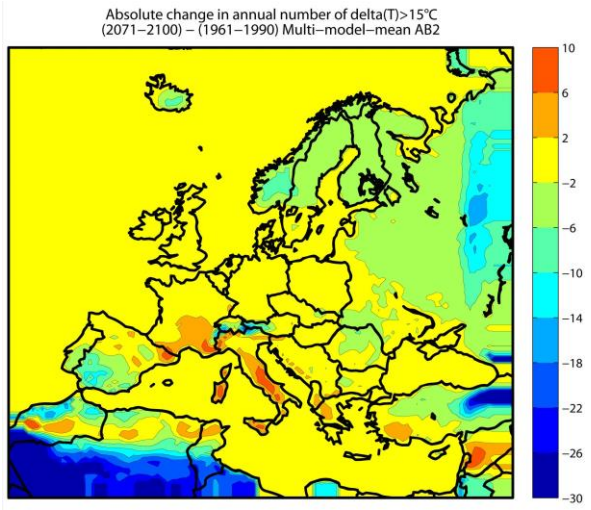

Fig. 2. Change in annual number of cases of temperature change in 6 hours by more than 15 °C

In north-eastern Europe and in the Alps, there is a general decrease in the number of rapid temperature changes. This is likely associated with a decrease in snow cover as, in the present climate, this promotes the formation of strong temperature inversions. In southern Europe, the patterns are more mixed. Where an increase is seen, such as over Italy, it is related to an increase in the average summertime diurnal temperature range. This, in turn, is likely caused by reduced cloudiness and soil moisture, which lead to a more variable radiation climate and less effective evaporative damping of temperature variations.

While qualitatively similar in many respects, the simulations based on the *Had* and *MPI* boundary data exhibit some marked quantitative differences. In northern Europe, Italy and Spain, the absolute values of both increases and decreases seem to be slightly more pronounced for *MPI* than for *Had*. Otherwise, the large changes near the southern and eastern boundaries, where the simulated climate is distorted by relaxation effects, are difficult to interpret.

Figure 3 shows the change in the annual integrated cold sum (<0 °C) between the periods 1961 - 1990 and 2071 - 2100. This variable is calculated based on daily values of maximum and minimum temperature so that the temperature change between these two values was assumed to be linear. The units of the variable are defined as °Kelvin hours (so changes can be quoted, more conveniently, in °C hours) and it is, as expected, dominated by wintertime changes. This index is a nonlinear function of both the length and the severity of the winter, with by far the largest present-day values (not shown) in the coldest (north-eastern) parts of the area (up to approximately 7×10^4 °C hours). For this reason, and because the simulated wintertime warming also increases from west to east, the largest decreases are seen in the north-eastern parts of the model domain.

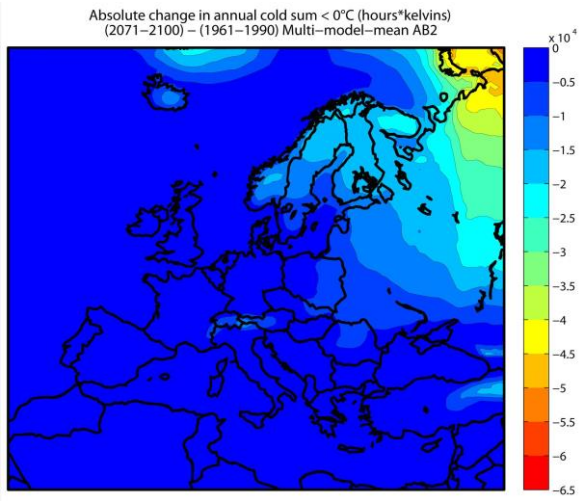

Fig. 3. Change in the annual cold sum (°C hours)

In Figure 4 the annual heat sum is plotted with a threshold temperature of 25 °C. The variable is calculated with the same daily data of maximum and minimum temperatures and has the same units [°C hours]. In the present climate the value of this parameter is very small for most of Europe, highest values reaching 6×10^4 in Spain (not shown). This spatial pattern is very similar compared with changes of the index (Fig. 4) and the relative increase is very high in central Europe. Because the sum is unaffected by days with the maximum temperature below 25 °C, and because the RCAO model has a slight tendency to underestimate the highest summer temperatures in northern Europe (Räisänen et al. 2003), both the simulated 20th century values and the changes in northern Europe are rather small in absolute terms. Much larger increases occur further south in Europe, the function of the index being nonlinear in the same way as the cold sum index. This index is also a good example of the dependence of the results on the driving GCM simulation. The larger summer warming in the *MPI* than in the *Had* simulations also leads to a larger increase in the heat sum in southern and central Europe.

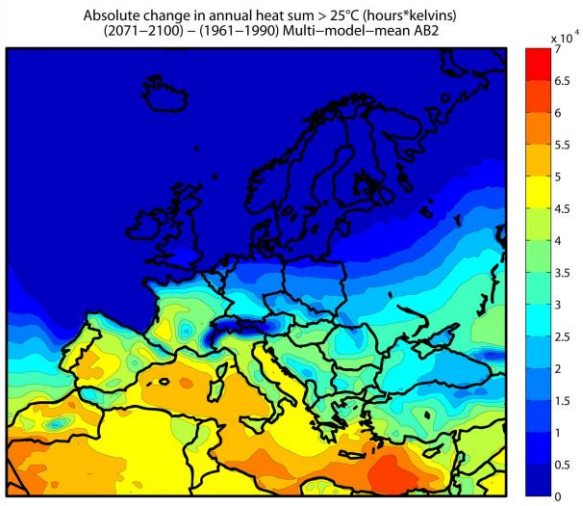

Fig. 4. Change in the annual heat sum (°C hours)

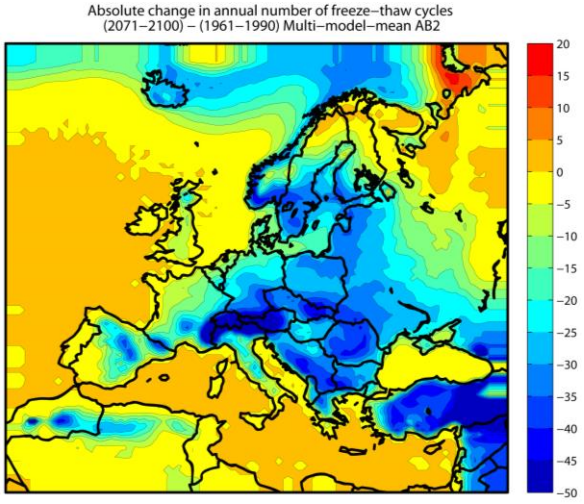

Fig. 5. Change in the number of 0 °C temperature crossings (annual)

As expected, increases in the heat sum mostly occur in the summer season. However, the warming of autumns also seems to contribute substantially to the annual sums in the southern Mediterranean area.

Figure 5 shows the change in the annual number of cases when the temperature crosses the freezing point of zero degrees. This variable is calculated from the 6-hourly temperature data. In the present climate this variable is close to zero in western and southern parts of Europe and up to 130 only in the mountainous regions (not shown). The fact that this variable increases towards south-western Europe and is therefore, quite significant.

Figure 6 shows the same result in the four individual simulations. Comparison of Figures 5 and 6 gives an impression on how much the simulations based on different emission scenarios and global models differ from each other and from the mean value.

The number of freeze-thaw cycles shows both seasonal and spatial variability, and this is illustrated in Figures 7a (winter) and 7b (spring); the contribution of summer and autumn is small for this variable. When looking at the annual maps most areas are bluish in colour, indicating fewer zero-crossings in the future. However, in the coldest, north-eastern parts of the integration area, the situation is not that simple.

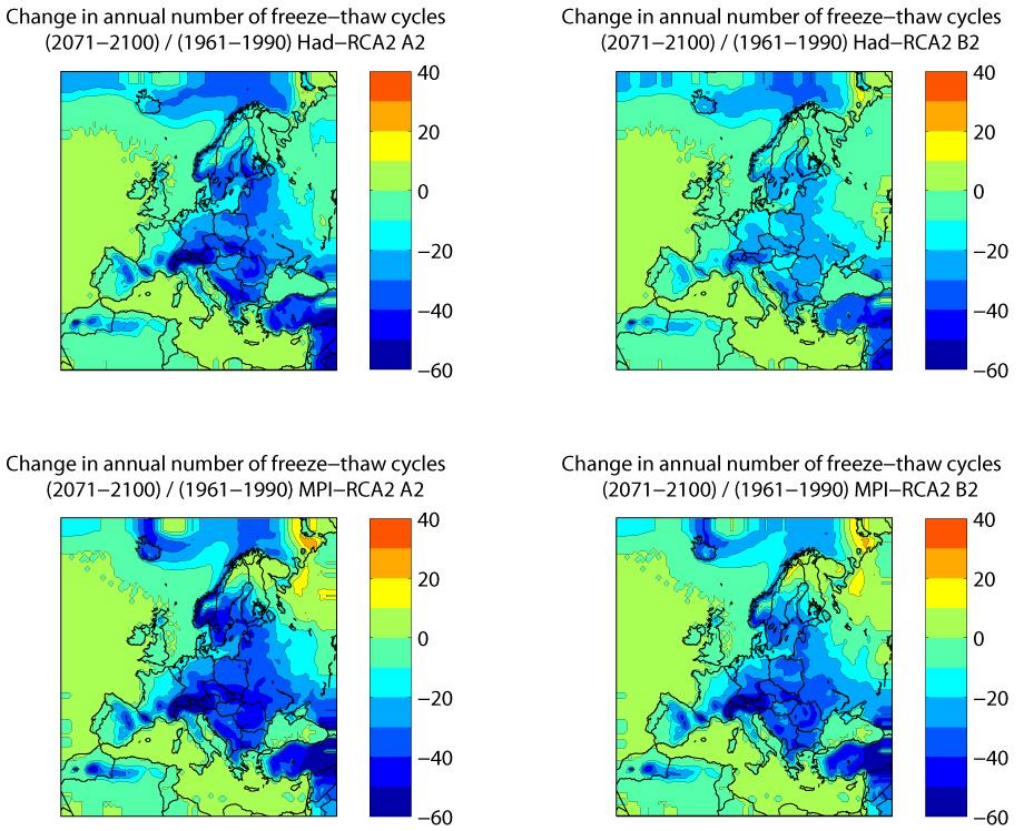

Fig. 6. Change in the number of 0 °C temperature crossings (annual) as simulated by using two different emission scenarios and two different global climate models

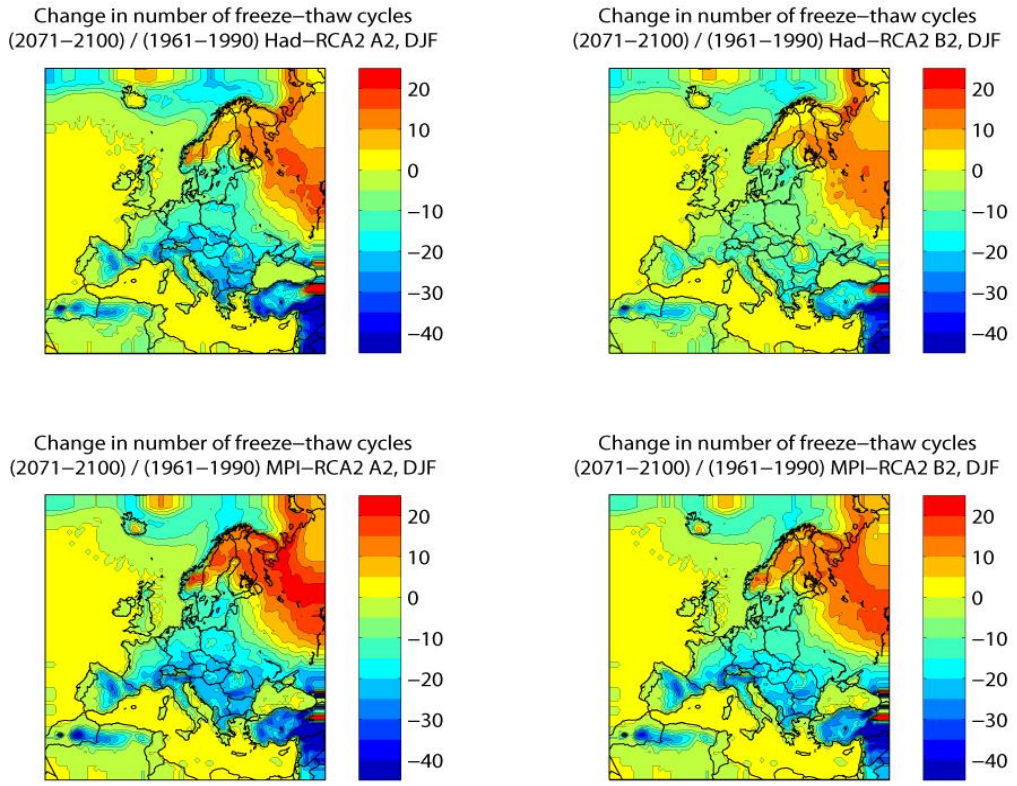

Fig. 7a. Change in the number of 0 °C temperature crossings in winter (Dec., Jan., Feb.)

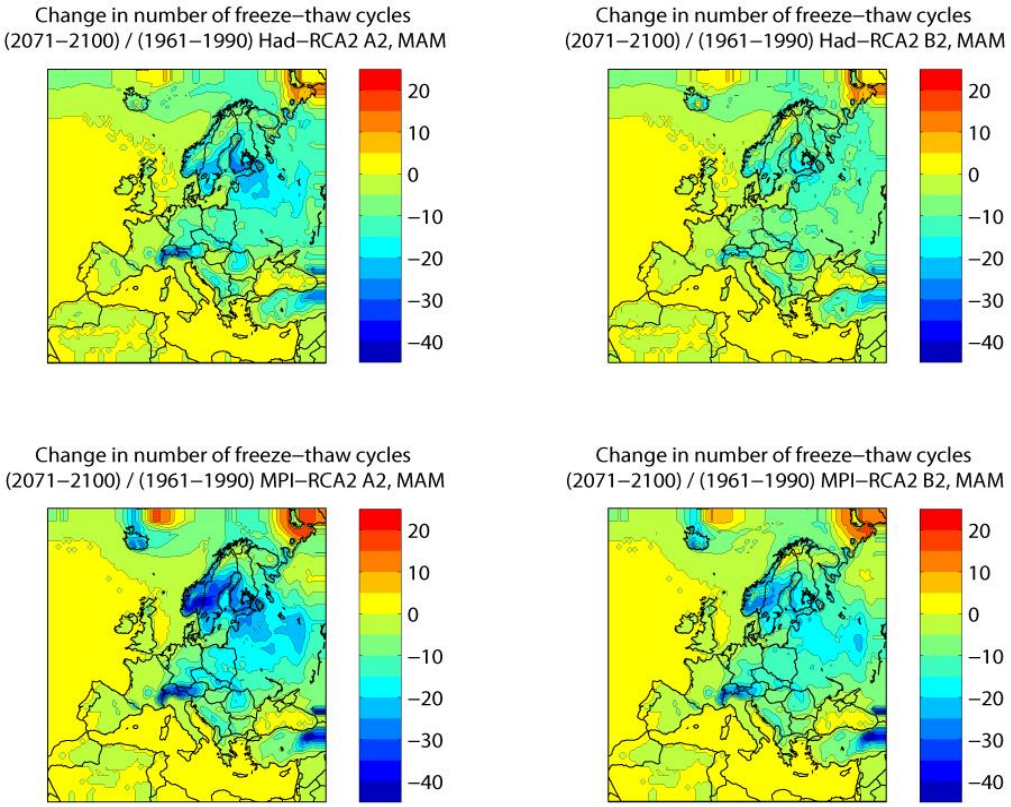

Fig. 7b. Change in the number of 0 °C temperature crossings in spring (Mar., Apr., May)

Here, in wintertime, the zero-crossings will increase (Fig. 7a), but in springtime they will decrease (Fig. 7b) in the same area. This is because of the climate conditions. In these areas, which are seen as the red belt in the figure 7a, the warming will make the winter temperatures to stay closer to zero in the future. To the northeast of this area, the temperatures will still be cold enough to keep the number of zero-crossing events relatively low, hence a smaller increase is seen there. In the spring, the belt of increase retards to the extreme northeast of the domain, and is replaced by marked decrease further to the southwest, particularly southern Finland and central Scandinavia, as well as in the Alps. There, the average spring temperatures are already in the present climate close to (or in the end of the spring, well above) zero; consequently a further warming of climate leads to fewer zero-crossings. Both of these findings are quite robust across all of the simulations.

Figure 8 shows the projected change in the annual precipitation amount. The present-day values are in the range of 300 to 2000 mm per year, so that the projected changes represent a very significant relative change, up to 50% in north-eastern Europe and down to -30% in the south (not shown).

In annual results, the borderline between increasing and decreasing precipitation is not well

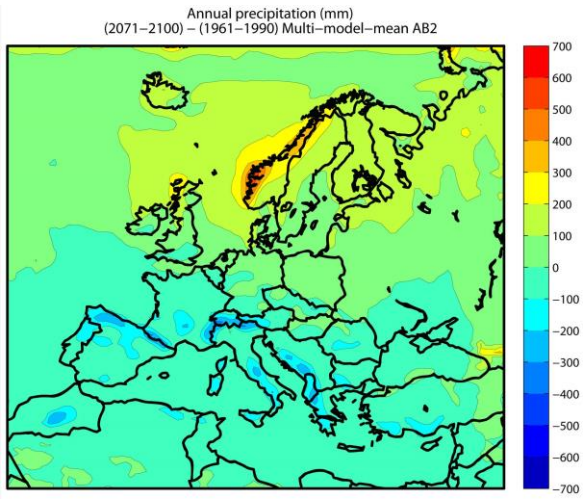

Fig. 8. Change in the annual precipitation.

defined in the *Had*-simulations. In the *MPI*-simulations, the contrast between southern and northern Europe is much sharper. The maps during the wintertime (not shown) look very much the same as those obtained from other simulations within the PRUDENCE (Prediction of Regional Scenarios and Uncertainties for Defining European Climate Change Risks and Effects [Christensen et al. 2007]) project, but the summertime maps seem to show greater

declines of precipitation in central Europe. Nevertheless, the general characteristics are all the same. In summer, the precipitation will decrease with the exception of the most northern areas (approximately to the north of 60°N; see Fig. 6 of Räisänen et al. 2004), and in winter precipitation will increase except for the southernmost areas near the Mediterranean. The differences in the precipitation change between the two driving models are partly related to different changes in the atmospheric circulation during the winter half-year; in particular, there is a strong increase in time-mean westerly flow in northern Europe in *MPI* that is absent from *Had* (Räisänen et al. 2004). Furthermore, the aforementioned larger increases in Atlantic Ocean surface temperatures in *MPI* than in *Had* also, most likely, contribute to the differences in precipitation change by providing a larger increase in the moisture content of air *(*Kendon et al. 2009).

4 Implications of the results regarding road networks

In this chapter implications from the maps presented in Section 3 are outlined. Effects on the road network - surface, bridges, drainage and maintenance are considered. We give a severity rating score in a scale of 1 (low) to 5 (high) for various effects. These scores are merely subjective estimates by the authors based on their expert evaluation of the consequences. More detailed estimates will be made in further ongoing EU-projects.

4.1 Change in the annual maximum temperature (Figure 1)

Regional patterns of the changes

- In all simulations the greatest change in the annual maximum temperature is observed in Central Europe, in France, in southern parts of Germany, northern Italy and in the Balkan region: 5 to 12 °C. In Western Europe the change is greater than in Eastern Europe. In the Mediterranean region and Southern UK the change is not so extreme: 4 to 8 °C. In Northern Europe, Northern UK and Ireland the change is limited to 1 to 6 °C.

Effects

- Asphalt roads will experience significant increases in rutting and deformation unless modifications are made to the surface materials in the future. One should most probably be able to adapt to the increase in rutting in roads where the pavement has a rehabilitation cycle of less than 20 to 30 years. On thin paved roads the effect also applies to the unbound bearing layers and road base as the softened pavement redistributes the stress caused by traffic loading less effectively than planned. Changing of the pavement material to a more rigid one should be made by the middle of the century on thin paved roads to avoid deformations.
- On concrete paved roads an increase of the joint openings and movements will be observed. Greater movement caused by thermal expansion can be expected and should be compensated by providing functioning construction joint solutions on bridge decking and concrete paved roads. These safety measures should be planned in advance on bridges with a long service life, i.e. one should ensure at construction stage that the structure has sufficient expansion capability to safely respond to the deformations that will result from predicted future temperature régimes. Some existing bridges may need to be retrofitted with such capability.

Severity

- We estimate that the financial and operational consequences will be 3 in Western Central Europe and 1 or 2 in other regions.

4.2 Annual number of events in which the change in air temperature within six hours is more than 15 °C (Figure 2)

Regional patterns of the changes

- In Italy, South Western France, possibly in Greece and on islands of the Western Mediterranean, the frequency of rapid air temperature changes will increase. In other regions this frequency will remain the same or decrease.

Effects

- The phenomenon contributes to forced stress loading by differential thermal expansion and contraction, particularly on brittle materials and structural parts with two different joining materials (concrete pavement, expansion joint etc.). A rapid change in air temperature does not necessarily correspond to a temperature change of the materials because of thermal intertia and possible exposure to sunlight. A more detailed analysis of this effect would, therefore require thermal models of the structures and more comprehensive climate model data including e.g. cloudiness.

Severity

- A significance of 2 is estimated for the countries listed above.

4.3 The change of annual cold sum (<0 °C) in h °C (Figure 3)

Regional patterns of the changes

- In Nordic countries and the Baltic countries the annual cold sum will significantly decrease: -15000…-20000 °C hours. In Southern Sweden and Poland the change is -5000…-10000 °C hours or less. In other regions the change is insignificant.

Effects

- The change presented in the graphs depicts an average change and not an extreme change (e.g. occurring once in 20 or 50 years). However, it is obvious that as the annual cold sum is an accumulated sum, the extreme values of the index can be expected to decrease. A quantification of extreme years cannot be made based on the results depicted here. The change in the annual cold sum has two explicit consequences a) frost penetration depth will change and b) the period of time when road structures are in a frozen state per annum will change. This is of major consequence in the Nordic and Baltic regions where reliance is placed on the strong, frozen road structures, historically available during winter, to access rural areas for (e.g.) forestry purposes. In addition in these areas, very thick pavement foundations are currently provided beneath the pavements of major highways in order to achieve frost protection. There is also an obvious effect on the existence of winter ice roads.
- North of the Arctic Circle, the present average annual cold sum is less than -40000 °C hours. In the average latitude of the Nordic countries the annual cold sums are between -20000 and -35000 °C hours. With a change of +15000…+20000 °C hours, the penetration depth of the frost at the Arctic Circle will decrease by approximately 20% and further to the south by up to 50%. If there is a corresponding change in the annual cold sum of those individual years having extremely cold conditions, one could, for example, permit thinner frost protection layers beneath newly constructed major highways provided other prerequisites (load capacity, drainage etc.) are ensured.
- The change of annual cold sum is largely due to a decrease in the winter length. This means that the decrease of annual cold sum affects the months during which the *rasputitsa* (the strong softening of the road body caused by a surplus of water due to snow and frozen ground melting) will occur and the decrease in the length of the periods in which heavy load transportation can be executed on low volume roads. A relevant example is that transportation of wood from forests to the major highways will be possible for shorter periods of time in the winter months. Some compensation can be expected because the end of autumn trafficking conditions will be later and the commencement of summer trafficking conditions earlier. However, in these seasons, load carrying capacity of the minor road network is not so great as during the fully frozen winter period, so the overall effect will be negative.
- The change in a limited area (Lapland) is significant. The affect is adverse concerning transportation.

Severity

- An overall significance of 2 is estimated for North Europe. However there are both positive and negative influences so, locally the significance could be 4.

4.4 The change in the annual heat sum in °C hours (Figure 4)

Regional patterns of the changes

- Except for mountainous areas (the Alps) the °C hours will increase significantly (3000 - 6000 °C hours) in the area south of the 50° N latitude. In the 40° N latitude (Spain, France) the change would be approximately 6000 - 7000 °C hours.

Effects

- The largest consequences will be observed between the 40° N and 50° N latitude lines, if no adaptations are made towards the use of deformation resistant surface materials. In such areas - if no adaptations are made and current materials will be used - the deformations will increase significantly. However, the change will occur gradually, enabling adaptation within regular pavement rehabilitation cycles. On roads with small traffic load and thin paved roads, the surface material will age more quickly than previously. On asphaltic roads the cracking and deformations of the supporting layer will increase. Selection of asphalts with lower penetration bitumens will readily address the rutting issue. An increase in top-down cracking is also suggested (Hoff and Lalagüe 2010) which may necessitate increased use of polymer modification of bituminous binders.
- Evaporation will increase during summer period benefiting roads through improved support conditions. Roadside vegetation can be expected to change and this should be managed responsively.

- The risk of erosion due to the accumulated effect of dehydrated ground and sudden rain showers will increase. The maintenance work on drainage system and gulley chambers will increase.

Severity

- A significance of 3 is estimated. Adaptation needs can be expected.

4.5 Change in number of freeze-thaw cycles (Figures 5 - 7)

Regional patterns of the changes

- The number of freeze-thaw cycles will decrease in all simulations except for the northernmost Europe, in particular Lapland.

Effects

- The reduction in number of freeze-thaw cycles (associated with a warmer climate) will mean a reduction in freezing-initiated cracking of pavements and other porous materials.
- In most regions of Europe the change is beneficial and will decrease the pace of winter surface material degradation. A change in the air temperature does not directly correspond to a change in the surface material temperature, but the change is similar.
- Porous asphalts will be more readily used in high latitudes where, formerly, frost damage and snow/ice clearance made their use questionable.

Severity

- ***A significance of 1 is estimated as the impacts will either be insignificant or beneficial. Adaptation will be possible by normal responsive maintenance procedures.***

4.6 Change in annual precipitation (Figure 8)

Regional patterns of the changes

- Annual precipitation will increase in the regions north of the 55th latitude, but it will decrease further to the south. In particular, the decrease will occur in mountainous areas. The absolute increase, shown by Fig. 8 in the coastal areas of Norway is large, but when one takes into consideration the relatively large current annual precipitation, the change is not so significant. However, the relative change is in the order of magnitude of 30% to 40% in many areas (not shown). A more significant effect is an increase of precipitation in a region stretching from Central Europe to Northern Europe and especially in regions bordered with the Atlantic Ocean, mountainous and elevated areas (only the MPI model). The increase of the annual precipitation is, based on the model results, mainly due to an increase of short-term heavy rain (Makkonen et al. 2007), i.e. increased storm intensity rather than number of rainfall events.

Effects

- A decrease in the annual precipitation, an increase in the intensity of hot weather and an increase in the number of temperate days will accumulatively affect, especially, the drainage of road structures and of surface layers. Subgrades can be expected to provide stronger road structures with longer overall lives (with the exception of surfacing, as described above). However, the effect is not only positive as the erosion susceptibility, due to heavy rain after dry spells, will increase and, especially in southern Europe, dust from unsealed roads can be expected to become more problematic. The most significant problems of erosion may be experienced on road side-slopes
- Where precipitation increases due to an increase in heavy rain spells, this will lead to road base water saturation, overloading of the drainage system, erosion of the subsurface soils and, hence in extreme cases, local cave-ins. Localised flooding may have a similar effect at low points in the road profile. The water saturation of natural slopes will also increase, leading to an increased risk of instability of roads located in sloping terrain.
- Correspondingly, water loading on bridges and the undermining of bridge piers due to fluvial erosion will increase. In extreme cases this could lead to bridge safety issues (Sibley 2009).

Severity

- In Northern Europe the effect is significant, 3 to 4 or even extreme 5. The increase in precipitation must be taken into consideration in advance planning, especially concerning structures that are difficult to replace, i.e. having a long design life. The required level of advance measures and optimal timing will be hard to predict unless systematic bridge- and route-specific risk assessments are made. In Southern Europe erosion of unpaved roads by gravel loss in dry weather or by water erosion in heavy storms after prolonged dry periods can be expected to increase.

5 Conclusions

Conclusions of the climate model results and their analysis are summarized in Table 1.

Table 1. Conclusions of the effects in a changing climate

Implication	*Where significant*	*Effects* *Severity*	*Adaptation needs*
Change in the annual maximum temperature	**Western Central Europe, Italy, Balkans**	**Rutting deformations expansion of joints** **Severity: 3**	**For roads adaptation with time** **Bridges: early adaptation**
Change in the number of events per annum in which the change of temperature within six hours is greater than 15 °C	**Mediterranean area from Greece to France**	**Forced deformation, service life of brittle materials, expansion joints** **Severity: 2**	**Bridges: early adaptation**
Change in the annual cold sum	**Nordic Countries, Baltic states**	**Frost penetration: positive effect** **Bearing capacity in wintertime (heavy transport)** **Severity: 2**	**Adaptation with time**
Change in the annual heat sum	**Mountainous areas, Spain, France**	**Deformations and cracking on asphaltic roads, vegetation and indirect erosion risk** **Severity: 3**	**Adaptation with time**
Change in number of freeze-thaw cycles	**Northernmost Europe**	**Lapland: negative, other regions beneficent** **Severity: 1**	**Adaptation with time**
Change in the annual precipitation	**North, Northwestern Atlantic coastal areas**	**Severity: 3…5**	**Timing of adaptation based on risk analysis**

Further studies should be made using the climate models, for example corresponding analysis could be made for the extreme events (Makkonen et al., 2007).

In this study, only variables that are directly obtained from the climate model simulation data were considered. The selected variables undoubtedly correlate with real problems on roads and, therefore, indicate the consequences of the global climate change on road networks in the study regions.

They are, however, only overall indicators of the factors that are important since the phenomenological models and the chosen threshold values are based on empiricism only. Therefore, studies should be initiated to utilize these data in specific applications of adaptation to climate change in the road infrastructure sector. These need to be done in close co-operation with the engineers aware of the practical problems to be expected.

An example of applying climate simulations for future adaptation and design is shown in Fig. 9. The relationship between frost depth and cumulative freezing degree-hours on roads can be represented by the following simplified Stefan equation (Yolder et al., 1975)

$$D_F = c\, F^{1/2} \qquad (1)$$

where

D_F is frost depth (cm)
F cold sum with respect to 0°C (°C h)
c empirical coefficient, for most soil types c≈1

In Fig. 9 the climate model data of the simulations on which Fig. 3 is based on is applied via Eq. (1) for the present (above) and the projected future climate (below). These results demonstrate the potential of using the data published in this report and available from climate modellers. The example in Fig. 9 also shows that some of the changes affecting the road networks in Europe can be quite significant within this century.

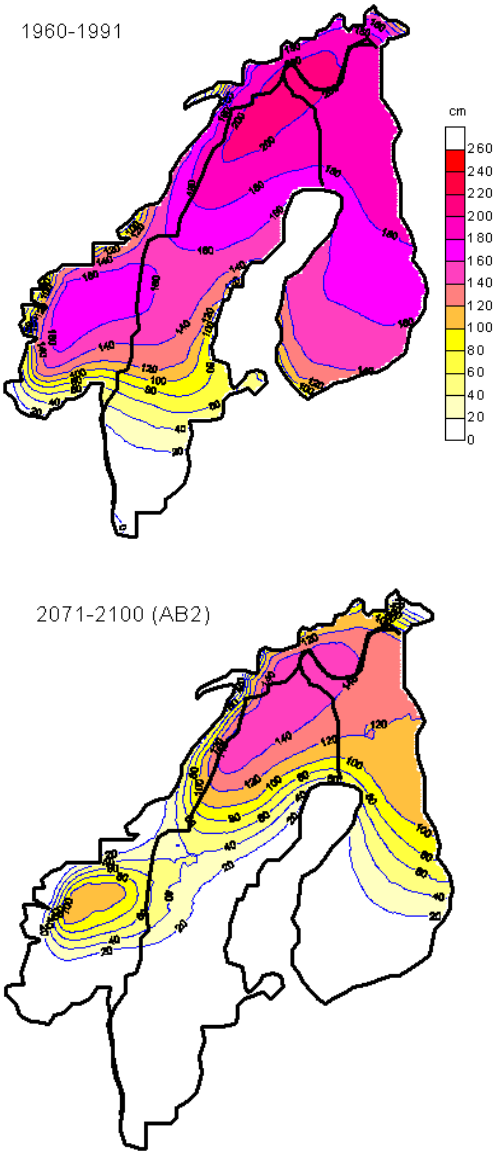

Fig. 9. Change of the maximum frost depth during an average year in the Nordic countries in areas which are kept clean of snow (roads, airfields etc.).

A more specific approach would be possible and should be considered in the future. It is quite feasible to combine a physical or a statistical model of a certain road infrastructure degeneration process with climate model data analysis. The simulation of that process could then proceed on a six hour basis over many decades. Such a technique would make it possible to simulate locally and in a process-specific way the degeneration with time and investigate in detail how different processes respond to the projected climate change. However, such an approach would necessitate having statistically valid pavement performance data for the type of road, subgrade and drainage system of interest.

Acknowledgements

This work was funded by the P2R2C2/Road ERA-NET project. It was also supported by the Academy of Finland. The climate model output data was produced by the Rossby Center of the Swedish Meteorological and Hydrological Institute.

References

Anon. 2008. Potential Impacts of Climate Change on U.S. Transportation. Transportation Research Board Special Report 290, National Academy of Sciences, USA, 298 p. ISBN 978-0-309-11306-9.

Bringfelt, B.; Räisänen, J.; Gollvik, S.; Graham, L.P.; Ullerstig, A. 2001. The land surface treatment for the Rossby Centre regional atmospheric climate model - version 2 (RCA2), *SMHI Reports Meteorology and Climatology*, 98, Swedish Meteorological and Hydrological Institute, 40 p.

Castro, M.; Gallardo, C.; Jylhä, K.; Tuomenvirta, H. 2007. The use of a climate-type classification for assessing climate change effects in Europe from an ensemble of regional climate models. *Clim. Change* 81, Supplement 1: 329–341.

Christensen, J.H.; Christensen, O.B. 2007: A summary of the PRUDENCE model projections of changes in European climate by the end of this century. *Clim. Change* 81: 7–30.

Döscher, R.; Willén, U.; Jones, C.; Rutgersson, A.; Meier, H.E.M.; Hansson, U. 2002. The development of the regional coupled ocean-atmosphere model RCAO. *Boreal Env. Res.* 7: 183–192.

Eerola, K.; Salmond, D.; Gustafsson, N.; Garcia-Moya, J-A.; Lönnberg, P.; Järvenoja, S. 1997. A parallel version of the HIRLAM forecast model: strategy and results. *Proc. 7th ECMWF Workshop on the use of parallel processors in meteorology*. World Sci. Publ., 134–143.

Gordon, C.; Cooper, C.; Senior, C.A.; Banks, H.; Gregory, J.M.; Johns, T.C.; Mitchell, J.F.B.; Wood, R.A. 2000. The simulation of SST, sea ice extent and ocean heat transport in a version of the Hadley Centre coupled model without flux adjustments, *Clim. Dyn*. 16: 147–166.

Hoff, I.; Lalagüe, A. 2010. *Analysis of pavement structural performance*, Report No. 7 from SINTEF to Pavement Performance and Remediation Requirements following Climate Change project, 24 p. (available at http://www.nottingham.ac.uk/~evzard/P2R2C2).

Jones, C.G.; Willén, U.; Ullerstig, A.; Hansson, U. 2004. The Rossby Centre Regional Atmospheric Climate Model, Part I: Model climatology and performance for the present climate over Europe, *Ambio* 33: 199–210.

Kendon, E.J.; Rowell, D.P.; Jones, R.G. 2009. Mechanisms and reliability of future projected changes in daily precipitation. *Clim. Dyn*. 35(2–3): 489–509.

Makkonen, L.; Ruokolainen, L.; Räisänen, J.; Tikanmäki, M. 2007. Regional climate model estimates for changes in Nordic Extreme events. *Geophysica* 43: 19–42.

Meehl, G.A.; Stocker, T.F.; Collins, W.D.; Friedlingstein, P.; Gaye, A.T.; Gregory, J.M.; Kitoh, A.; Knutti, R.; Murphy, J.M.; Noda, A.; Raper, S.C.B.; Watterson, I.G.; Weaver A.J.; Zhao, Z.-C. 2007. Global Climate Projections. In: *Climate Change 2007: The Physical Science Basis. Contribution of Working Group I to the Fourth Assessment Report of the Intergovernmental Panel on Climate Change* [Solomon, S., D. Qin, M. Manning, Z. Chen, M. Marquis, K.B. Averyt, M. Tignor and H.L. Miller (eds.)]. Cambridge University Press, Cambridge, United Kingdom and New York, NY, USA, p. 747–845.

Meier, H.E.M. 2001. On the parameterization of mixing in 3D Baltic Sea models, *J. Geophys. Res*. 106: 30997–31016.

Meier, H.E.M.; Döscher, R.; Coward, A.C.; Nycander, J.; Döös, K. 1999. Rossby Centre regional ocean climate model: model description (version 1.0) and first results from the hindcast period 1992/1993, *SMHI Reports Oceanography 26*, Swedish Meteorological and Hydrological Institute, Norrköping, Sweden, 102 p.

Nakićenović, N.; Alcamo, J.; Davis, G.; de Vries, B.; Fenhann, J.; Gaffin, S.; Gregory, K.; Grubler, A.; Jung, T.Y.; Kram, T.; La Rovere, E.L.; Michaelis, L.; Mori, S.; Morita, T.; Pepper, W.; Pitcher, H.; Price, L.; Raihi, K.; Roehrl, A.; Rogner, H-H.; Sankovski, A.; Schlesinger, M.; Shukla, P.; Smith, S.; Swart, R.; van Rooijen, S.; Victor, N.; Dadi, Z. 2000. *Emission Scenarios*. A Special Report of Working Group III of the Intergovernmental Panel on Climate Change, IPCC, Cambridge University Press, 599 p.

Räisänen, J. 2001. The impact of increasing carbon dioxide on the climate of northern Europe in global climate models (in Finnish with English abstract and figure and table captions), *Terra* 113: 139–151.

Räisänen, J.; Hansson, U.; Ullerstig, A.; Döscher, R.; Graham, L.P.; Jones, C.; Meier, M.; Samuelsson, P.; Willén, U. 2003. GCM driven simulations of recent and future climate with the Rossby Centre coupled atmosphere - Baltic Sea regional climate model RCAO. *SMHI Reports Meteorology and Climatology* 101, Swedish Meteorological and Hydrological Institute, 61 p.

Räisänen, J.; Hansson, U.; Ullerstig, A.; Döscher, R.; Graham, L.P.; Jones, C.; Meier, M.; Samuelsson, P.; Willén, U. 2004. European climate in the late 21st century: regional simulations with two driving global models and two forcing scenarios, *Clim. Dyn*. 22: 13–31.

Rockner, E.; Bengtsson, L.; Feichter, J.; Lelieved, J.; Rodhe, H. 1999. Transient climate change simulations with a coupled atmosphere-ocean GCM including the tropospheric sulfur cycle, *J. Clim*. 12: 3004–3032.

Semenov, V.A.; Bengtsson, L. 2002. Secular trends in daily precipitation characteristics: greenhouse gas simulation with a coupled AOGCM, *Clim. Dyn*. 19: 123–140.

Sibley, A. 2009, Analysis of extreme rainfall and flooding in Cumbria 18–20 November 2009, Weather, 65(11): 287–292.

Solomon, S.; Qin, D.; Manning, M.; Chen, Z.; Marquis, M.; Averyt, K.B.; Tignor, M.; Miller, H.L. (eds.). 2007. Climate Change 2007: The Physical Science Basis. Contribution of Working Group I to the Fourth Assessment Report of the Intergovernmental Panel of Climate Change, IPCC, Cambridge Univ. Press. 996 p.

Yoder E. J.; and Witczak M. W. (1975) "Principles of Pavement Design", John Wiley & Sons. 711 p.